Picrotoxin Inhibition Mechanism of a γ-Aminobutyric Acid$_A$ Receptor Investigated by a Laser-Pulse Photolysis Technique†

Latha Ramakrishnan and George P. Hess*

Department of Molecular Biology and Genetics, 216 Biotechnology Building, Cornell University, Ithaca, New York 14853-2703

Received October 25, 2004; Revised Manuscript Received January 6, 2005

ABSTRACT: The γ-aminobutyric acid$_A$ (GABA$_A$) receptor, a major inhibitory neurotransmitter receptor, belongs to a family of membrane-bound proteins that regulate signal transmission between ∼10^{12} cells of the nervous system. It plays a major role in many neurological disorders, including epilepsy. It is the target of many pharmacological agents, including the convulsant picrotoxin. Here, we present the mechanism of inhibition by picrotoxin of the rat α1β2γ2L GABA$_A$ receptor investigated using rapid kinetic techniques in combination with whole-cell current recordings. The following new results were obtained by using transient kinetic techniques, the cell-flow method and the laser-pulse photolysis (LaPP) technique with a microsecond to millisecond time resolution. (i) The apparent dissociation constant of picrotoxin for the open-channel form of the receptor was ∼5 times higher than that of the closed-channel form. (ii) Picrotoxin increased the channel-closing rate constant (k_{cl}) approximately 4-fold, while the rate constant for channel opening (k_{op}) remained essentially unaffected. (iii) The mechanism indicates that picrotoxin binds to an allosteric site of the receptor with higher affinity for the closed-channel form than for the open-channel form and thereby inhibits the receptor by decreasing 4-fold its channel-opening equilibrium constant [$\Phi_I^{-1} = k_{op(I)}/k_{cl(I)}$]. (iv) The mechanism further indicates that compounds that bind with equal affinity to the picrotoxin-binding site on the open-channel form of the receptor and the closed-channel form will not affect the channel-opening equilibrium and can, therefore, displace picrotoxin and prevent inhibition of the GABA$_A$ receptor by picrotoxin. Such compounds may be therapeutically useful in counteracting the effects of compounds and diseases that unfavorably affect the channel-opening equilibrium of the receptor channel.

The γ-aminobutyric acid type A (GABA$_A$) receptor, a major inhibitory ligand-gated ion channel in the central nervous system (*1*), belongs to a family of membrane-bound neurotransmitter receptors responsible for transmission of signals at the junctions (synapses) between many of the ∼10^{12} cells of the mammalian nervous system (*2*). Upon binding their specific neurotransmitter, GABA, the GABA$_A$ receptors form transient chloride-conducting transmembrane channels (*1, 3*). GABA$_A$ receptors are generally assembled from a combination of α-, β-, and γ-subunits, with the most common subunit assembly being α1β2γ2 (*1, 3*). This receptor composition was used in the experiments reported here.

GABA$_A$ receptors are known to possess a variety of allosteric binding sites from which a number of drugs can modulate receptor function (*1*). A plant convulsant, picrotoxin, which inhibits the GABAergic inhibitory postsynaptic current, is one such allosteric ligand. The molecular composition of picrotoxin is a 1:1 molar mixture of picrotin and picrotoxinin (Figure 1). Picrotoxinin is the toxic component of picrotoxin (*4*). Picrotoxin also inhibits other anion-conducting neurotransmitter receptors, such as the GABA$_C$ (*5*), glycine (*6*), and glutamate-gated Cl^- channels (*7*), as well as cation-conducting serotonin receptors (*8*). Convulsions are also caused by mutations of the GABA$_A$ receptor linked to forms of epilepsy (*9*−*11*), a disease affecting 50 million people worldwide (*12*). The dysfunction of one of these mutated GABA$_A$ receptors (*9*) has recently been investigated by rapid kinetic techniques (*13*). It was shown that the dysfunction of an epilepsy-linked GABA$_A$ receptor is due to a decreased channel-opening equilibrium constant (*13*). In the case of the nicotinic acetylcholine receptor

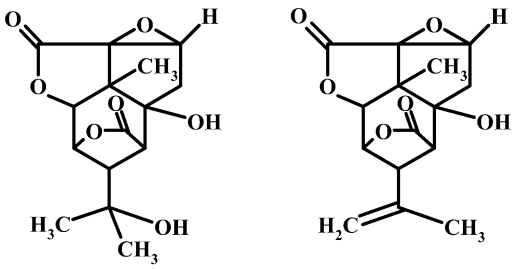

FIGURE 1: Structures of picrotin (A) and picrotoxinin (B) that are present as a 1:1 molar mixture (*48*) in picrotoxin.

† These studies were funded by a U.S. Public Health Service National Institutes of Health grant (NS08527) awarded to G.P.H. and by an Epilepsy Foundation Postdoctoral Fellowship, through the generous support of the American Epilepsy Society and Milken Family Foundation, awarded to L.R.

* To whom correspondence should be addressed. E-mail: gph2@cornell.edu. Telephone: (607) 255-4809. Fax: (607) 255-6249.

[1] Abbreviations: HEK293, human embryonic kidney cells; GABA, γ-aminobutyric acid; LaPP, laser-pulse photolysis; α-CNB-caged GABA, *N*-(α-carboxy-2-nitrobenzyl)-GABA; nAChR, nicotinic acetylcholine receptor.

10.1021/bi0477283 CCC: $30.25
Published on Web 05/18/2005

(nAChR), it has been shown that compounds such as cocaine and MK-801 [(+)-dizocilpine] that inhibit this receptor by decreasing its channel-opening equilibrium (*14*−*16*) can be used to obtain combinatorially synthesized RNA ligands that can displace these noncompetitive inhibitors without themselves inhibiting the receptor (*17*). These RNA ligands bind with equal affinity to the open- and closed-channel forms of the receptor. Therefore, they do not affect the channel-opening equilibrium and consequently do not inhibit receptor function (*17*−*20*). Knowledge of the inhibition mechanism of the convulsant picrotoxin may, therefore, be important for the rational design of therapeutic anticonvulsants. The mechanism by which the $GABA_A$ antagonist, picrotoxin, inhibits the receptor is the subject of this study.

Previously proposed mechanisms of the inhibition of the $GABA_A$ receptor by picrotoxin were based mainly on electrophysiological measurements (*21*) and on the effects of the neurotransmitter GABA on the onset and reversal of inhibition by picrotoxin (*21*−*23*). Electrophysiological studies of the action of picrotoxin on $GABA_A$ receptors expressed in different cells, varying from neurons to recombinant receptor systems (*21*−*24*), have shown that the mechanism of picrotoxin inhibition of this receptor is a complex phenomenon. The inhibitor has been considered to be a simple open-channel blocker (*7*, *21*), a mixed/noncompetitive inhibitor (*22*−*24*), or a noncompetitive inhibitor that binds to an allosteric site to stabilize a closed or desensitized state of ligand-gated ion channels (*22*, *24*−*26*). Detailed analysis of single-channel current recordings suggested a more complex scheme (*22*). Neither picrotoxin nor its more active component picrotoxinin had any effect on the conductance of single-channel events mediated by $GABA_A$ receptors (*22*, *24*). Single-channel current recordings showed that picrotoxin decreased the channel-opening frequency in a manner compatible with the stabilization of an agonist-bound closed state that perhaps corresponds to a desensitized conformation of the receptor (*22*, *27*, *28*). The precise mechanism of picrotoxin inhibition is believed to be still unknown (*22*−*25*).

Recently, the existing techniques for investigations of receptor mechanisms have been supplemented by rapid chemical kinetic approaches, the cell-flow (*29*) and the laser-pulse photolysis (LaPP) techniques (*30*, *31*), suitable for measurements of receptor-mediated reactions on cell surfaces in the microsecond to millisecond region (reviewed in ref *30*). The LaPP technique utilizes a photolabile, biologically inactive, caged precursor of a neurotransmitter that is equilibrated with the receptors on the cell surface (*30*). A single laser pulse liberates the free neurotransmitter [in this case GABA (*32*)] in the microsecond time region (*32*). The released neurotransmitter binds to the receptor and activates the opening of receptor channels. The resulting macroscopic current is measured by the whole-cell current-recording technique (*33*). Such caged compounds have been shown to be suitable for transient kinetic investigations of receptor mechanisms (*30*, *31*, *34*) and for studying the inhibition of the nicotinic acetylcholine receptor by noncompetitive inhibitors such as cocaine (*14*) and MK-801 (*15*). This report describes rapid kinetic studies of picrotoxin inhibition of the $\alpha1\beta2\gamma2L$ $GABA_A$ receptor transiently transfected in HEK293 (human embryonic kidney) cells.

MATERIALS AND METHODS

GABA and picrotoxin were purchased from Sigma (St. Louis, MO). Plasmid cDNAs for the rat $GABA_A$ receptors were a gift from P. H. Seeburg (Max Planck Institute for Medical Research, Heidelberg, Germany). In these plasmids, the cDNAs encoding the $\alpha1$, $\beta2$, and $\gamma2L$ (long splice variant) rat $GABA_A$ subunit proteins are individually cloned into pRK-5 mammalian expression vectors (BD Biosciences, San Diego, CA). Effectene transfection reagent was purchased from Qiagen (Valencia, CA).

Cell Culture and Transient Transfection. HEK293 cells (American Type Cell Culture, Manassas, VA) were transiently transfected with rat $GABA_A$ $\alpha1$, $\beta2$, and $\gamma2L$ cDNAs in a 1:1:3 ratio using the Effectene transfection reagent (Qiagen). The cells were cotransfected with cDNA encoding the green fluorescent protein (pGreenLantern plasmid, Life Technologies, Gaithersberg, MD) to detect transfected cells (*35*). The culture and transfection of the HEK293 cell line were done as described previously (*36*). HEK293 cells were grown in 25 cm^2 canted-neck cell culture flasks (Corning, Corning, NY) containing the growth medium DMEM (Dulbecco's modified Eagle's medium, high glucose, Invitrogen GibcoBRL, Grand Island, NY) supplemented with 10% FBS (fetal bovine serum, Invitrogen GibcoBRL) and antibiotics (100 U of penicillin and 100 μg of streptomycin, both from Sigma). Cells were passaged weekly (after reaching 80−90% confluence), and $\sim2 \times 10^5$ cells were seeded in 35 mm Falcon dishes (Fisher Scientific) in 10% FBS and 90% DMEM containing 1% penicillin/streptomycin. The transfection reaction mixture was added to the cells 24 h after they were passaged. After 6 h, the transfection mixture was removed from the cells, which were then washed once with 1× phosphate-buffered saline (Invitrogen GibcoBRL) followed by the addition of 2 mL of 1% FBS in the DMEM growth medium. The cells were replated the next day in 35 mm Falcon dishes and were used for electrophysiological measurements up to 48 h from the time of transfection.

Electrophysiology. For both the cell-flow (*29*) and LaPP (*30*, *31*) experiments, the recording glass pipets were pulled from borosilicate glass (World Precision Instruments Inc., Sarasota, FL) using a two-stage puller (L/M 3 P-A, Adams & List, Westbury, NY) and a flame polisher (MF-83, Narishige, Tokyo, Japan). Typical pipet resistances were 2−4 MΩ, and the series resistances were 1−4 MΩ for whole-cell current measurements. Series resistance compensation of 60−70% was used in the whole-cell current recording measurements (*33*). The bath buffer contained 145 mM sodium chloride, 5 mM potassium chloride, 2 mM calcium chloride, 1.5 mM magnesium chloride, 10 mM *N*-(2-hydroxyethyl)piperazine-*N*′-2-ethanesulfonic acid, and 10 mM glucose; the pH was adjusted to 7.4 using 5 N sodium hydroxide. The electrode solution contained 140 mM cesium chloride, 10 mM tetraethylammonium chloride, 2 mM magnesium chloride, 10 mM ethylene glycol tetraacetic acid, and 10 mM *N*-(2-hydroxyethyl)piperazine-*N*′-2-ethanesulfonic acid; the pH was adjusted to 7.4 using cesium hydroxide (50 wt % solution in water). An Axopatch 200B amplifier (Axon Instruments, Union City, CA) with a 1−5 kHz low-pass filter was used for the current recordings. Signals were acquired using the pClamp 8.0.1 software packet (Axon Instruments). Whole-cell current-recording data were digi-

tized at 0.5−2 kHz. LaPP data were digitized at 20−50 kHz using the Digidata 1320A instrument (Axon Instruments). Data were analyzed off-line on a personal computer, and the time constants for the rising and decaying phases for the whole-cell current were obtained by using a nonlinear least-squares fitting program with Microcal (Northampton, MA) Origin version 3.5. All measurements were carried out at pH 7.4, 22 °C, and a transmembrane voltage of −60 mV. Data from each cell were normalized to the response measured with 100 μM GABA. All solutions used in the experiments were prepared on the day of measurements. The GABA (5 mM) stock solution can be stored at 4 °C for several weeks. The freshly prepared picrotoxin (1 mM) stock solution can be stored at 4 °C for a few weeks. The α-CNB-caged GABA [*N*-(α-carboxy-2-nitrobenzyl)-GABA (*32*), Molecular Probes, Eugene, OR] stock solution (5 mM) was stored at −80 °C and protected from light. During measurements, the caged GABA solution was kept on ice in brown tubes to minimize hydrolysis.

Cell-Flow and Laser-Pulse Photolysis. The whole-cell current-recording technique developed by Hamill et al. (*33*) was used in conjunction with cell-flow (*29*) and LaPP (*30*) methods. The cell-flow technique, which allows rapid ligand application as well as a method for making a desensitization correction of the observed whole-cell current, has been described previously (*29*). Briefly, a cell (ca. 10−20 μm diameter) in the whole-cell current-recording configuration was placed ca. 100 μm from the porthole (diameter of ca. 150 μm) of a U-tube made from stainless steel high-performance liquid chromatography (HPLC) tubing (Hamilton, Reno, NV). The flow rate of the neurotransmitter solution emerging from the flow device was typically ∼1 cm/s. A freshly prepared dilution of the 5 mM GABA stock solution flowed over the cell in the absence or presence of varying concentrations of the inhibitor (1 mM picrotoxin stock solution was used for preparing different dilutions) to determine the affinity of picrotoxin for the closed- and open-channel forms of the receptor. In cell-flow experiments with 100 μM GABA, the observed rise time of the whole-cell current to its maximum value, characteristic of the time for GABA to equilibrate with the cell surface receptors, was 60−100 ms. Receptor desensitization during this time can be significant. In the cell-flow method, the observed current was, therefore, corrected, as described previously (*29*), for desensitization that occurs during the time it takes GABA to equilibrate with the receptors on the cell surface. If a fraction of current remained after the desensitization reaction had gone to completion (usually less than 5% of the total current), it was subtracted from the observed current before correction. Cells were allowed to recover for 2 min after each experiment via the flow of the bath buffer solution (composition given above) over the cell, for a time sufficient to guarantee full resensitization of the receptors (*37*).

The LaPP experiments were performed as described previously (*30*). In brief, a photolabile, biologically inactive precursor of a neurotransmitter (*30*, *38*), called a "caged neurotransmitter", is used. After equilibration of the receptors on the cell surface with the caged neurotransmitter using the cell-flow device (*29*), the free neurotransmitter was released by irradiation in the microsecond time region with a pulse of laser light. The resulting current, due to the binding of neurotransmitter leading to the opening of transmembrane channels, was measured. Several caging groups have been developed for the neurotransmitters (*38*). For this work, the photolabile precursor, α-CNB-caged GABA (*32*), was used. It was used previously to investigate the mechanism of the rat hippocampal $GABA_A$ receptors (*34*) and of the recombinant rat wild type as well as a mutated $GABA_A$ receptor linked to one form of epilepsy (*13*). The cell was equilibrated with either the caged compound alone or a mixture of the caged GABA and picrotoxin for 400 ms (at 25 μM α-CNB-GABA) or 1 s (at 100 μM α-CNB-GABA) before the laser irradiation. Photocleavage of the caged GABA was initiated by a pulse of laser light from a nitrogen laser (λ = 337 nm, pulse duration = 10 ns; COMPEX 101, Lambda Physik AG, Goettingen, Germany) coupled to a 300 μm core diameter optical fiber (Laser Components, Santa Rosa, CA), which delivered the laser light to the cell. The unattenuated laser energy was ∼400−500 μJ, which released 5 ± 1 and 23 ± 7 μM free GABA from 25 and 100 μM caged GABA, respectively.

In a typical experiment, a cell in the whole-cell configuration was first rapidly perfused with 100 μM GABA using the cell-flow device (*29*) and the current was recorded and corrected for receptor desensitization. After 2 min, the LaPP experiments were performed. After every LaPP experiment, a control cell-flow experiment was conducted with 100 μM GABA to monitor for possible changes in receptor activity or laser-induced damage of the receptors or the cell. Data obtained from cells with a significant change (>20%) in the control current after photolysis were discarded. To determine the concentration of GABA released from the α-CNB-caged GABA, the maximum current amplitude observed in the LaPP experiment was compared to that obtained in the cell-flow experiment performed with same cell used in the LaPP experiments. This information and the known relationship between GABA concentration and current amplitude obtained in the cell-flow experiments were used to calculate the concentration of GABA released in LaPP experiments (reviewed in ref *30*). Cell-flow experiments were also conducted with the highest concentration of caged GABA (100 μM) used in the LaPP experiments together with 25 μM GABA to determine whether the presence of α-CNB-caged GABA changed the current amplitude measured in its absence. The maximum current amplitudes observed in these experiments were the same in either the presence or absence of α-CNB-caged GABA (data not shown), indicating that the α-CNB-caged GABA was biologically inert when concentrations of ≤100 μM were used. When α-CNB-caged GABA at a concentration greater than 100 μM was co-applied with 25 μM GABA, the caged compound inhibited the GABA-evoked whole-cell current. The inhibition of the $GABA_A$ receptor by α-CNB-caged GABA (*32*) under certain circumstances has been reported previously (*39*). The flash/flow system was controlled using pClamp 8.0.1 (Axon Instruments).

RESULTS AND DISCUSSION

Effect of Picrotoxin on the Concentration of Open Receptor Channels. We determined the effect of picrotoxin on the concentration of open receptor channels, when the receptor was either mainly in the closed-channel conformation (5 μM GABA, ○ symbols in Figure 2A) or in the open-channel conformation (100 μM GABA, △ symbols in Figure 2A).

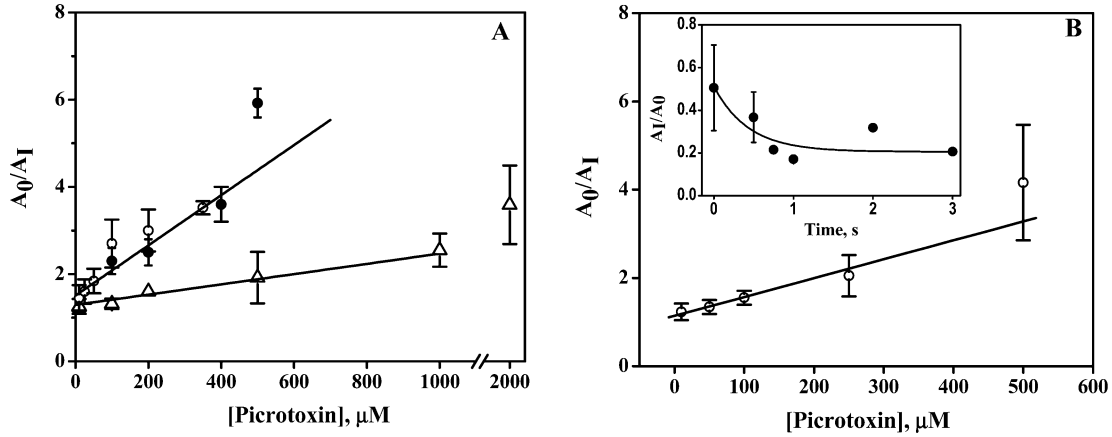

FIGURE 2: Inhibition by picrotoxin of the $\alpha1\beta2\gamma2$L $GABA_A$ receptor transiently transfected in HEK293 cells. The ratio of the maximum current amplitudes in the absence, A_0, and in the presence, A_I, of the inhibitor picrotoxin was plotted as a function of the inhibitor concentration. Each data point is the mean of at least three measurements made with three different cells in the bath buffer (composition given in Materials and Methods) at −60 mV, pH 7.4, and 22 °C. (A) Experiments were carried out with varying concentrations of picrotoxin that was co-applied, using a cell-flow device made of a U-tube (*29*), with 5 μM (○) or 100 μM (△) GABA. The apparent K_I values for picrotoxin of 174 ± 27 μM (at 5 μM GABA) and 852 ± 35 μM (at 100 μM GABA) were determined from the best fit (solid line) of the data plotted according to eq 1 (Appendix). The filled symbols (●) represent the measurements obtained from LaPP experiments where ∼5 μM free GABA was released from 25 μM α-CNB-caged GABA that was preincubated with the cell for 400 ms together with different concentrations of the inhibitor. (B) Inhibition by picrotoxin of the slowly equilibrating site of the receptor was assessed by preincubating the receptors on the cell surface with picrotoxin for 1 s followed by co-application of the same concentration of the inhibitor with 100 μM GABA. Ratios of the maximal current amplitudes in the absence, A_0, and presence, A_I, of picrotoxin, measured using the cell-flow technique, are plotted (○) as a function of the inhibitor concentration. The solid line is the best fit of the data to eq 1 (Appendix); the value of $K_{I,app}$ was found to be 234 ± 31 μM. The inset shows A_I/A_0 measured as a function of preincubation time using 100 μM GABA with 500 μM picrotoxin. The solid line represents the result obtained from nonlinear regression analysis of the data according to eq 2 (Appendix). The rate constant for the slow inhibition process, k_{obs}'', is calculated to be 2.3 ± 1.1 s^{-1}, as described in the text.

The ratio of the maximum current amplitude [corrected for receptor desensitization (*29*)] in the absence (A_0) or the presence (A_I) of picrotoxin as a function of picrotoxin concentration (Figure 2A and 2B) was measured. To determine the dissociation constant ($K_{I,app}$) for a noncompetitive inhibitor such as picrotoxin from its binding site, the data in panels A and B of Figure 2 are fitted by eq 1 (*40*) in the Appendix.

As the GABA concentration was increased from 5 to 100 μM (Figure 2A), the fraction of receptors in the open-channel form increased by more than ∼6-fold from 0.14 at 5 μM GABA to 0.85 at 100 μM GABA, as calculated from the K_S value of 34 ± 13 μM and the Φ^{-1} value of 10 ± 1 obtained previously (*13*) using eq 3B (Appendix). If the inhibitor picrotoxin bound only to the open channel, as deduced from some previous experiments (*7*, *21*), as the GABA concentration is increased the receptor affinity for picrotoxin would increase, corresponding to a decrease in $K_{I,app}$ for picrotoxin. Consequently, the slope of the data obtained at 100 μM GABA (△ symbols in Figure 2A) plotted according to eq 1 (Appendix) would increase. However, the opposite results were obtained. In Figure 2A, the slope of the line obtained at 100 μM GABA is less than the slope of the line obtained at 5 μM GABA. The decrease in the slope obtained at the high GABA concentration corresponds to an ∼5-fold increase in $K_{I,app}$ and, therefore, to a decrease in the affinity of the receptor in the open-channel form for picrotoxin. Moreover, the increase in $K_{I,app}$ from 174 ± 27 to 852 ± 35 μM (Figure 2A), in the range of GABA concentrations that was used (from 5 to 100 μM), corresponds closely to the increasing fraction of receptors in the open-channel form. These results indicate that picrotoxin binds at least ∼5 times more strongly to the closed-channel forms of the receptor (A, AL, and AL_2) than to the open-channel form ($\overline{AL_2}$) (Figure 6). The measurements that indicate picrotoxin binds with much higher affinity at a low concentration (5 μM) of GABA, when the receptor is mainly in the closed-channel conformation, than at a high concentration (100 μM) of GABA can give the impression that GABA can alleviate picrotoxin inhibition, suggesting that picrotoxin inhibition has a competitive component (*23*, *24*, *41*). The experiments depicted in Figure 3A, however, indicate that GABA concentrations ∼100 times higher than its apparent dissociation constant (K_S = 34 μM) do not overcome picrotoxin inhibition. This is in contrast to what is expected for competitive inhibition (*42*).

Effect of Preincubation of the Receptor with Picrotoxin. The inhibition process described so far is what happens when the noncompetitive inhibitor is co-applied with the agonist. However, besides this fast inhibition process, which occurs during the time the ligands equilibrate with the cell surface receptors in the cell-flow technique [∼60−100 ms (*29*)], another slower process was observed in the inhibition of the muscle-type nAChR by MK-801 (*15*). Therefore, the effect of the duration of preincubation of the $GABA_A$ receptor with picrotoxin on the whole-cell current was investigated (Figure 2B, inset). The cells were preincubated with picrotoxin before the agonist GABA was co-applied with the inhibitor, using a cell-flow device made of a modified U-tube (*43*), to study the effect of preincubation duration on the extent of inhibition (Figure 2B, inset). At 5 μM GABA, preincubation with picrotoxin for up to 5 s (data not shown) did not increase the inhibition compared to the simple co-application with GABA (○ symbols in Figure 2A). However, at 100 μM GABA, preincubation with picrotoxin for 1 s (○ symbols in Figure 2B) significantly increased the inhibition over that obtained with the simultaneous GABA application (△ symbols in Figure 2A). The apparent inhibition dissociation constant ($K_{I,app}$) decreased from 852 ± 35 to 234 ± 31 μM,

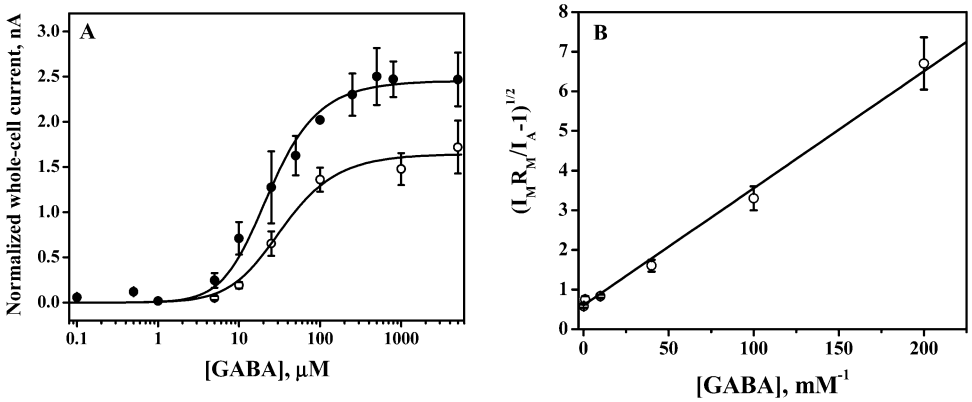

FIGURE 3: Effect of 500 μM picrotoxin on the GABA dose−response curve recorded in the bath buffer at −60 mV, pH 7.4, and 22 °C from HEK293 cells transiently expressing the rat $\alpha1\beta2\gamma2L$ $GABA_A$ receptor. The data were normalized to the whole-cell current corrected for desensitization (*29*), obtained in the presence of 100 μM GABA. Each data point is an average of two to six measurements made with two to four cells. (A) The parameters used to compute the solid line [according to the nonlinear form of eq 3A (Appendix)] for the filled symbols (●) representing the GABA dose−response curve in the presence of GABA alone, $I_M R_M$, K_S, and Φ, are 3 ± 0.1 nA, 35 ± 3 μM, and 0.23 ± 0.1, respectively. The parameters used to compute the solid line for the open symbols (○) representing the GABA dose−response curve in the presence of GABA and 500 μM picrotoxin, $I_M R_M$, K_S, and Φ, are 2.27 ± 0.2 nA, 49 ± 7 μM, and 0.38 ± 0.1, respectively. (B) The GABA dose−response curve in the presence of 500 μM picrotoxin, which was co-applied with GABA, is presented in panel A (○ symbols) and is replotted here in the linear form according to eq 3A (Appendix). The solid line is the best fit of the data using eq 3A (Appendix). The values for parameters $I_M R_M$ and K_S of 2.27 nA and 49 μM, respectively, were used; the value of the channel-closing equilibrium constant Φ_I was obtained from the ordinate intercept and is equal to 0.36 ± 0.01.

corresponding to an ~4-fold increase in the inhibitor affinity compared to that obtained when 100 μM GABA and picrotoxin were co-applied.

The rate constant for the slow inhibition process can be determined from the plot of A_I/A_0 versus preincubation duration (Figure 2B, inset). Cells were perfused with picrotoxin (500 μM) alone for the indicated time; subsequently, 100 μM GABA was co-applied with 500 μM picrotoxin. Approximately 50% of the inhibition process went to completion within the mixing time of picrotoxin with the receptors on the cell surface (~60−100 ms). A second much slower process went to completion within ~1 s. The data (Figure 2B, inset) were fitted using eq 2 (*15*) in the Appendix. The $A_{I(t=\infty)}/A_0$ term in eq 2 was set to 0.21 (the value after preincubation for 3 s), and from a nonlinear regression analysis of the data (Figure 2B, inset) using eq 2 (Appendix), $A_{I(t=0)}/A_0$ and k_{obs}'' were estimated to be 0.31 ± 0.08 and 2.3 ± 1.1 s^{-1}, respectively. The results are similar to those obtained for the slow inhibition process of the muscle-type nAChR by MK-801 (*15*).

The GABA dose−response curve recorded in the presence of 500 μM picrotoxin is presented in Figure 3A. The value of the equilibrium GABA dissociation constant (K_S) was determined to be 49 ± 7 μM in the presence of 500 μM picrotoxin, compared to its value of 35 ± 3 μM obtained in the absence of picrotoxin for the rat $GABA_A$ receptor (Figure 3A; *13*) using the cell-flow method (*29*). Such a right shift in the equilibrium dose response for GABA in the presence of picrotoxin has been reported previously (*24*). The channel-closing equilibrium constant ($\Phi = k_{cl}/k_{op}$) in the presence of picrotoxin was evaluated from the GABA dose−response curve replotted in linear form using eq 3 (Appendix). From the ordinate intercept of the solid line in Figure 3B and using eq 3 (Appendix), a value for Φ_I of 0.36 ± 0.01 was obtained. This corresponds to a channel-opening equilibrium constant, Φ_I^{-1}, of 2.8 ± 0.5, a value that is much lower than the value of 10 ± 1 for the channel-opening equilibrium constant (Φ^{-1}) for the $GABA_A$ receptor in the absence of picrotoxin determined previously (*13*). A decrease in Φ_I^{-1} in the presence of picrotoxin indicates that the inhibitor reduces receptor function by decreasing the channel-opening equilibrium constant. Either an increase in k_{cl} (channel-closing rate constant) or a decrease in k_{op} (channel-opening rate constant) could lead to a decrease in Φ^{-1}, which equals k_{op}/k_{cl}. To further understand the effect of this antagonist on Φ^{-1}, we used the LaPP technique that has a 100-fold better time resolution than the cell-flow method (*30*). Additional essential information about the effect of the inhibitor on k_{op} and k_{cl} and, therefore, on the channel-opening equilibrium constant was obtained from these studies.

Effect of Picrotoxin on the Rates of Channel Opening and Closing. Whole-cell currents obtained from HEK293 cells transiently expressing the $GABA_A$ receptors on photolysis of αCNB-caged GABA at various concentrations of picrotoxin, using the LaPP technique, are shown in Figure 4A. The whole-cell current decreases with an increase in picrotoxin concentration at 5 μM (Figure 4A) or 23 μM (Figure 4B) released GABA. The rising phase of the current in the LaPP experiments (Figure 4) follows a single-exponential rise for 85% of the reaction in all the measurements, and k_{obs}, the observed first-order rate constant for the current rise time at different picrotoxin concentrations, was determined from a nonlinear fitting using eq 4 (*30*) (Appendix).

The effect of picrotoxin on k_{obs} (Figure 5) indicates that the inhibition of the receptor by this antagonist can be ascribed to a decrease in the channel-opening equilibrium constant ($\Phi^{-1} = k_{op}/k_{cl}$) as a result of the inhibitor's higher affinity for its allosteric site on the closed-channel form (AIL_2) than for the site on the open-channel form ($\overline{AIL_2}$, Figure 6). At the low concentration of released GABA (5 μM) and with pre-incubation of the receptors with picrotoxin for 400 ms, k_{obs} increases with increasing inhibitor concentration, and at 1 mM picrotoxin, it reaches a value that is ~3 times the value obtained in the absence of picrotoxin (Figure 5A). It should be noted that k_{obs} does not increase

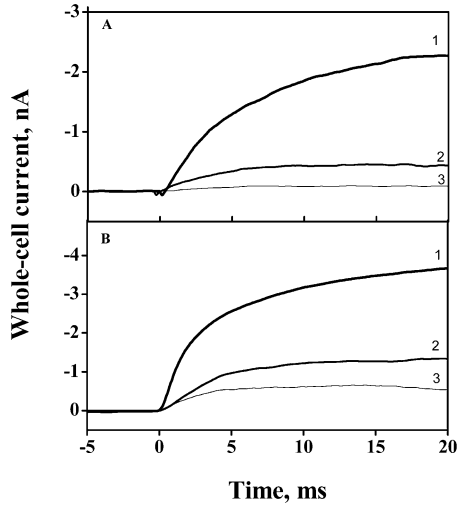

FIGURE 4: Whole-cell currents generated from laser-pulse photolysis of α-CNB-caged GABA, with HEK293 cells transiently transfected with the rat α1β2γ2L $GABA_A$ receptor at −60 mV, pH 7.4, and 22 °C in bath buffer. (A) Currents induced by release of 5 μM GABA from 25 μM α-CNB GABA in the absence (1) and presence of 500 (2) or 750 μM (3) picrotoxin. The laser was fired at time 0 after the cells were preincubated with the α-CNB-caged GABA and picrotoxin for 400 ms. The rising phase of the current is fitted by a single exponential using eq 4 (Appendix) (*30*). The values of the observed first-order rate constant for the current rise (*30*) of the whole-cell currents, k_{obs}, in traces 1−3 were determined to be 115 ± 1, 281 ± 2, and 322 ± 7 s^{-1}, respectively, and the maximum current amplitudes were 2394, 464, and 96 pA, respectively. (B) Currents induced by the release of 23 μM GABA from 100 μM α-CNB-GABA in the absence (1) and presence of 500 (2) or 1000 μM (3) picrotoxin. The laser was fired at time 0 after the cells were preincubated with the α-CNB-caged GABA and picrotoxin for 1 s. The observed first-order rate constants for the rise of the whole-cell currents in traces 1−3 are 325 ± 3, 224 ± 1, and 350 ± 15 s^{-1}, respectively, and the maximum current amplitudes are 3252, 1366, and 643 pA, respectively.

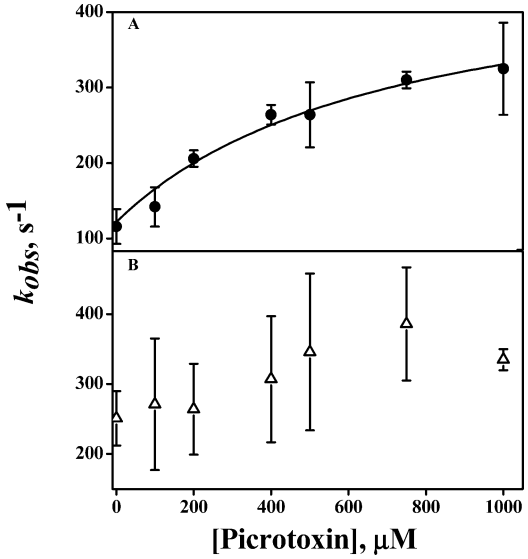

FIGURE 5: Effect of picrotoxin on k_{obs} for the current rise time determined using the LaPP technique (*30*) at −60 mV, pH 7.4, and 22 °C in bath buffer. Each data point represents two to four measurements, with each measurement made with a different cell. The observed first-order rate constant was obtained from the rising phase of the whole-cell current (eq 4, Appendix) generated by 5 (●) or 23 μM (△) released free GABA in the absence and presence of different concentrations of picrotoxin. The laser was fired at time 0 after the cells were preincubated with the α-CNB-GABA and picrotoxin for 400 ms in panel A and for 1 s in panel B. The solid line in panel A represents the best fit according to eq 6 (Appendix; *15*). The values for k_{cl}, k_{op}, and K_S were taken to be 113 s^{-1}, 1183 s^{-1}, and 34 μM, respectively (*13*). The apparent value of k_{op}' $\{=k_{op}[[L]/([L] + K_S)^2]\}$ is 19 s^{-1} at this GABA concentration. A nonlinear least-squares fitting program was used to obtain the values of $k_{cl(I)}$ (472 ± 67 s^{-1}) and $\overline{K}_I$ (718 ± 252 μM) and to construct the solid line.

linearly with increasing picrotoxin concentrations but reaches a limiting value (Figure 5A). At 750 μM picrotoxin, k_{obs} reaches a value ∼3 times (310 ± 11 s^{-1}) that obtained in the absence of picrotoxin (113 ± 9 s^{-1}) and remains approximately the same at picrotoxin concentrations up to 1 mM (325 ± 61 s^{-1}; Figure 5A). k_{obs} as a function of picrotoxin concentration can be quantitatively described by eq 6 (Appendix), and this is consistent with the observed nonlinear dependence of k_{obs} on picrotoxin concentration (Figure 5A). From a nonlinear least-squares fit of the data in Figure 5A (the solid line in Figure 5A was constructed by using eq 6 in the Appendix) and by using the experimentally obtained value for k_{cl} of 113 s^{-1} (*13*), the values of the rate constant for channel closing of the receptor−inhibitor complex [$k_{cl(I)}$] and the dissociation constant for dissociation of picrotoxin from the open-channel receptor form ($\overline{K}_I$) (Figure 6) were estimated: $k_{cl(I)}$ = 472 ± 67 s^{-1} and $\overline{K}_I$ = 718 ± 252 μM. The apparent value of k_{op}' $\{=k_{op}[L/(L + K_S)]^2\}$ determined from the values of 1183 s^{-1} and 34 μM for k_{op} and K_S, respectively (*13*), was taken to be 19 s^{-1} at this low released GABA concentration (5 μM).

At high GABA concentration (Figure 5B), the effect of picrotoxin on $k_{op(I)}$ is determined by equilibrating the receptors with the inhibitor for 1 s. In the presence of 5 μM GABA, the fraction of receptors in the open-channel form is 0.14 (eq 3A in the Appendix), and the value of k_{obs} for the current rise reflects primarily the rate constant for channel closing [$k_{cl(I)}$], according to eq 7 (*44*) (Appendix). In the presence of high concentrations (23 μM) of released GABA (Figure 5B), the k_{obs} value for the current rise time represents a sum of k_{cl} and k_{op}, the rate constant for channel opening (eq 6 in the Appendix). The effect of different concentrations of picrotoxin on $k_{op(I)}$ is obtained by subtracting the $k_{obs(I)}$ values obtained using the same concentration of picrotoxin at 5 μM released GABA (Figure 5A) from those obtained at 23 μM released GABA (Figure 5B). Increasing concentrations of picrotoxin had no significant effect on the value of $k_{op(I)}$ (Figure 5B). These results indicate that the inhibitor picrotoxin increases ∼4-fold the channel-closing rate constant while the channel-opening rate constant remains essentially unchanged. According to eq 9 (Appendix), when the rate constant for channel opening remains largely unaffected in the presence of the inhibitor (Figure 5), the ratio of the channel-opening equilibrium constant in the absence of the inhibitor to that in the presence of the inhibitor (Φ^{-1}/Φ_I^{-1}) is obtained from the ratio of the channel-closing rate constant in the presence of the inhibitor to that in the absence of the inhibitor [$k_{cl(I)}/k_{cl}$]. A value of 2.4 for the channel-opening equilibrium constant in the presence of the inhibitor [Φ_I^{-1} = $k_{op(I)}/k_{cl(I)}$] obtained from the LaPP experiments shown in Figure 5 using eq 9 (Appendix) is essentially in agreement with the value of 2.8 ± 0.5 obtained from the cell-flow experiments shown in Figure 3. Unlike cell-flow experiments,

the LaPP experiments give the k_{op} and k_{cl} values that determine the channel-opening equilibrium constant.

Mechanism of Inhibition by Picrotoxin. The channel-blocking mechanism predicts that as the concentration of open channels increases, the affinity of the receptor for picrotoxin also increases. Picrotoxin binds with an ~5-fold greater affinity to the closed-channel form than to the open-channel form (Figure 2A). These results are inconsistent with a mechanism in which picrotoxin can inhibit the receptor only by entering the receptor channel after it has opened and blocking it, i.e., the channel-blocking mechanism suggested previously (*21*). The results in Figure 2 also indicate that the picrotoxin reaction is independent of preincubation duration when the receptor is predominantly in the closed-channel form but not when the open-channel form predominates (Figure 2B). The effect of preincubation duration on the extent of inhibition at high GABA concentrations (Figure 2B) indicates the presence of both a fast and a slow inhibition process. When the receptors are predominantly in the closed-channel form, only the fast inhibition process seems to contribute to the receptor's inhibition. This suggests that the inhibitor reacts more rapidly with the closed-channel form of the $GABA_A$ receptor than with the open-channel form. How the binding site associated with the open-channel form, which binds picrotoxin ~5 times less strongly than the binding site associated with the closed-channel form, differs cannot be determined from the transient kinetic experiments. In the case of MK-801 inhibition of the nAChR, by using the LaPP technique Grewer et al. (*15*) have shown that the receptor is inhibited by MK-801 by an increase in the channel-closing rate constant without essentially an effect on the channel-opening rate constant. This leads to a decrease in the channel-opening equilibrium constant. Thus, the current observed when the receptor is exposed to the activating ligand in the presence of the inhibitor is decreased (*15*). In this study of the mechanism of inhibition of the $GABA_A$ receptor by picrotoxin, further experiments using the LaPP technique were conducted in an effort to understand the mechanism of inhibition of the receptor.

Can the shift of the channel-opening equilibrium to the closed-channel form in the presence of the inhibitor account for the reduction of the whole-cell current in the presence of picrotoxin and, therefore, receptor inhibition? According to eq 9 (Appendix), when the inhibitor does not affect k_{op} (Figure 5B), we obtained a value for Φ^{-1}/Φ_I^{-1} of 4.2 using the channel-closing rate constant determined from the LaPP experiments in the presence [$k_{cl(I)}$] (Figure 5A) or absence (k_{cl}) (*13*) of the inhibitor. For the proposed mechanism (Figure 6), the principle of microscopic reversibility (*45*) requires that the ratio of the inhibition constant for the open-channel form to that of the closed-channel form of the receptor ($\overline{K_I}/K_I$) be equal to the ratio of the channel-opening equilibrium constant in the absence to that in the presence of the inhibitor (Φ^{-1}/Φ_I^{-1}). The values for $\overline{K_I}/K_I$ of 4.1 and for Φ^{-1}/Φ_I^{-1} of 4.2 are obtained from the LaPP experiments (Figure 5).

The LaPP results in Figure 5 indicate that the picrotoxin-induced increase in $k_{cl(I)}$ without a concomitant change in $k_{op(I)}$ accounts for the decrease in the channel-opening equilibrium constant and for the inhibition by picrotoxin. Single-channel currents recorded from $GABA_A$ receptors in outside-out patches from mouse spinal cord neurons (*46*) have previously shown that picrotoxin decreases the mean open time (τ_o) of the receptor channel. The channel-closing rate constant, k_{cl}, is inversely proportional to the mean open time of the channel. Therefore, the results reported here, obtained by transient kinetic techniques, are in agreement with the single-channel data reported by Twyman et al. (*46*). The LaPP technique gives the additional information that k_{op} is essentially not affected by picrotoxin (Figure 5B). Therefore, the increase in k_{cl} caused by picrotoxin without a change in k_{op} indicates a decrease in the channel-opening equilibrium.

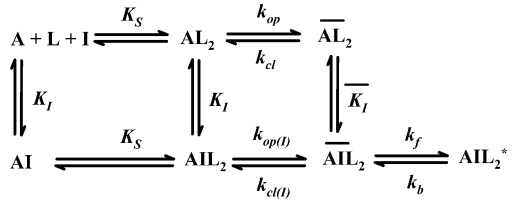

FIGURE 6: Minimum mechanism for the activation and inhibition of the $GABA_A$ receptor based on cell-flow (*29*) and LaPP (reviewed in ref *30*) measurements. A represents the active non-desensitized receptor form, L the neurotransmitter GABA, and I the inhibitor picrotoxin. AIL_2 represents the complexes in which the inhibitor is bound to the closed-channel form of the receptor. $\overline{AIL_2}$ represents the inhibitor-bound open-channel form of the receptor, and AIL_2* represents the nonconducting form of $\overline{AIL_2}$. K_S is the dissociation constant for the receptor−neurotransmitter complex, whereas K_I and $\overline{K_I}$ are the observed inhibitor dissociation constants of the closed-channel (A, AL, and AL_2) and open-channel ($\overline{AL_2}$) forms of the receptor, respectively. Φ is the equilibrium constant between the closed- and open-channel forms of the receptor (*49*, *50*) and is equal to k_{cl}/k_{op}, where k_{cl} is the rate constant for channel closing and k_{op} is the rate constant for channel opening. The corresponding channel-closing and channel-opening rate constants for the inhibitor-bound receptor channel are represented as $k_{cl(I)}$ and $k_{op(I)}$, respectively. k_f and k_b are the rate constants for interconversion between the open-channel form with the inhibitor bound ($\overline{AIL_2}$) and its nonconducting form, (AIL_2)*. It is assumed that the K_I values for all the closed-channel forms (A, AL, and AL_2) are the same. The transitions to desensitized receptor forms are not shown.

The results presented here (Figure 5) indicate the existence of a regulatory (inhibitory) site on the $GABA_A$ receptor that does not affect the opening rate of the ion channel but can increase the channel-closing rate and, therefore, results in a decrease in the channel-opening equilibrium. This inhibits the efficiency of the $GABA_A$ receptor and will affect signal transmission between cells. In the case of neurotransmitter receptors, equilibrium between active (open-channel) and inactive (closed-channel) conformations exists (Figure 6). The observation that noncompetitive inhibition of the $GABA_A$ receptor is brought about by changing the channel-opening equilibrium unfavorably is new. The mechanism of receptor activation and inhibition shown in Figure 6 indicates that the effect of noncompetitive inhibitors can be reversed by finding compounds that compete with the inhibitor but bind with equal or higher affinity to the open-channel form. These compounds are not expected to affect the channel-opening equilibrium unfavorably but can displace the inhibitor (*17*). Such an approach has been shown to be effective in the case of inhibition of the nAChR by cocaine (*17*−*20*), which inhibits this receptor by a mechanism (*14*−*16*, *19*) similar to the one described here for picrotoxin. The

regulatory site mechanism indicated here (Figure 6) suggests the possibility of finding therapeutic agents that compete with picrotoxin for the regulatory site but do not inhibit channel opening and signal transmission, and hence would be useful in alleviating the toxic convulsive effect of the inhibitor picrotoxin on the $GABA_A$ receptor. The existence of combinatorially synthesized RNA polymers that bind with higher affinity to an allosteric site on the open-channel form of the $GABA_A$ receptor than on the closed-channel form, and hence alleviate picrotoxin inhibition, has recently been reported (*47*).

CONCLUSIONS

The conclusions derived from this study are as follows. Picrotoxin binds to an allosteric site on the receptor, as suggested previously (*22*, *23*), and inhibits channel opening in a noncompetitive manner (*22*, *23*). The new information obtained by the measurements presented here follows. (i) Picrotoxin binds to the open-channel form of the receptor with an ~5-fold lower affinity than to the closed-channel form. Support for this conclusion is drawn from the following observations. When the receptor is mainly in the open-channel form, inhibition requires an ~5-fold higher concentration of picrotoxin than when it is mainly in the closed-channel form (Figure 2A). This observation has previously given the impression that there is a competitive component to picrotoxin inhibition (*23*, *24*, *41*). (ii) Picrotoxin inhibits the receptor's response to GABA by increasing the rate constant for channel closing (Figure 5A), but does not have an apparent effect on the rate constant for channel opening (Figure 5B). This ~4-fold increase in $k_{cl(I)}$ without a change in $k_{op(I)}$ decreases the channel-opening equilibrium constant and accounts for the observed inhibition of the receptor (Figure 6). The effect of picrotoxin on the lifetime of the open channel, a measure of the rate constant for channel closing (k_{cl}), has been noticed previously (*46*). However, transient kinetic methods, in particular the LaPP technique developed in this laboratory (*30*, *31*), allow one to determine not only k_{cl} but also the channel-opening rate constant (k_{op}) and, therefore, the channel-opening equilibrium constant. (iii) The ability to determine both of these rate constants led to the new conclusion that picrotoxin exerts its inhibitory effect by decreasing the channel-opening equilibrium constant ($\Phi^{-1} = k_{op}/k_{cl}$) of the $GABA_A$ receptor by a factor of 4. (iv) The insights obtained from the mechanism proposed suggested a search should be made for compounds that bind to the picrotoxin site without affecting the channel-opening equilibrium. These compounds can displace picrotoxin and thereby alleviate receptor inhibition by picrotoxin. This approach has been used successfully in alleviating the inhibition of the muscle and neuronal nAChRs by the abused drug cocaine (*17*−*20*). This drug inhibits the nAChR also by decreasing its channel-opening equilibrium (*14*, *18*, *19*). Similarly, knowledge of the mechanism presented here for the inhibition of the $GABA_A$ receptor by picrotoxin (Figure 6) led to the successful development of compounds that can alleviate the inhibition due to the unfavorable channel-opening equilibrium induced by picrotoxin (*47*). Can the same compounds also alleviate the unfavorable channel-opening equilibrium of a mutated $GABA_A$ receptor (*13*) linked to a certain form of epilepsy (*9*)?

ACKNOWLEDGMENT

We thank Professor P. H. Seeburg (Max Planck Institute for Medical Research) for the cDNAs encoding the α1, β2, and γ2L subunits of the rat $GABA_A$ receptor and Dr. Kyle Gee (Molecular Probes) for the *N*-(α-carboxy-2-nitrobenzyl)-GABA. L.R. thanks Susan Coombs for editorial help.

APPENDIX

The apparent dissociation constant ($K_{I,app}$) of the inhibitor picrotoxin is determined using the cell-flow method (*29*) for whole-cell current recording and eq 1 (*40*).

$$\frac{A_0}{A_I} = 1 + \frac{[I]}{K_{I,app}} \tag{1}$$

where A_0 and A_I represent the maximum current in the absence and presence of various inhibitor concentrations ([I]), respectively.

$$\frac{A_I}{A_0}(t) = \frac{A_{I,t=0}}{A_0}\exp(-k_{obs}''t) + \frac{A_{I,t=\infty}}{A_0} \tag{2}$$

where $A_{I,t=\infty}$ is the current amplitude in the presence of inhibitor after a long preincubation time, $A_{I,t=0}$ is the initial value of the current amplitude in the presence of inhibitor, and k_{obs}'' is the rate constant for the slower inhibition process (*15*).

$$(I_M R_M I_A^{-1} - 1)^{1/2} = \Phi^{1/2} + \Phi^{1/2} K_S [L]^{-1} \tag{3A}$$

a linear version (*29*) (eq 3A) of the dose−response curve for the neurotransmitter, GABA, where I_M is the current due to 1 mol of open receptor channels. R_M represents the number of moles of receptors in the cell membrane. For practical purposes, we take $I_M R_M$ to be the maximum current corrected for receptor desensitization (*29*) obtained in the presence of a saturating GABA concentration (5 mM). I_A is the whole-cell current corrected for receptor desensitization. K_S is the GABA dissociation constant, [L] the GABA concentration, and Φ the channel-closing equilibrium constant.

$$F_{\overline{AL_2}} = \frac{[L]^2}{([L] + K_S)^2\Phi + [L]^2} \tag{3B}$$

$F_{\overline{AL_2}}$ is the fraction of open-channel receptor forms (*29*) calculated from the values of K_S and Φ (eq 3A) obtained from the LaPP experiments with the wild-type $GABA_A$ receptor (*13*).

$$A_t = A_{max}[1 - \exp(-k_{obs}t)] \tag{4}$$

A_t is the measured current at time t and A_{max} the maximum observed current in a LaPP experiment (*44*). k_{obs} is the observed first-order rate constant for the current rise (*44*).

$$k_{obs} = k_{cl} + k_{op}\left(\frac{[L]}{[L] + K_S}\right)^2 \tag{5}$$

the relationship (eq 5) between the observed rate constant

for the current rise k_{obs}, and k_{op}, k_{cl}, and the ligand dissociation constant K_S.

$$k_{obs} = k_{cl}\left(\frac{\overline{K_I}}{\overline{K_I} + [I]}\right) + k_{cl(I)}\left(\frac{[I]}{[I] + \overline{K_I}}\right) + k_{op}\left(\frac{[L]}{[L] + K_S}\right)^2 \quad (6)$$

The relationship between k_{obs} and rate constants k_{op} and k_{cl} for an inhibitor that binds to both the open- and closed-channel forms of the receptor and the ligand-binding steps are fast compared to the channel-opening and -closing steps (*15*). Equation 6 has been derived according to the reaction scheme in Figure 6 (*14*, *15*), where K_I and $\overline{K_I}$ are the equilibrium dissociation constants of the inhibitor for the closed- and open-channel forms of the receptor, respectively, and $k_{cl(I)}$ is the channel-closing rate constant in the presence of the inhibitor.

At low GABA concentrations, the k_{obs} value obtained from the current rise time reflects the channel-closing rate constant (*16*; reviewed in ref *30*).

$$k_{obs} = k_{cl}\left(\frac{\overline{K_I}}{\overline{K_I} + [I]}\right) \quad (7)$$

The channel-opening rate constant in the presence of the inhibitor, $k_{op(I)}$, can be described by the following equation (*16*).

$$k_{op(I)} = \left[k_{op}\left(\frac{[L]}{[L] + K_S}\right)^2\right]\left[\frac{K_I}{[I] + K_I}\right] \quad (8)$$

$$\frac{k_{op}}{k_{cl}}\left[\frac{k_{op(I)}}{k_{cl(I)}}\right]^{-1} = \frac{k_{cl(I)}}{k_{cl}} = \frac{\Phi^{-1}}{\Phi_I{}^{-1}} \quad (9)$$

where $k_{op(I)}$ and $k_{cl(I)}$ are the rate constants for channel opening and closing, respectively, in the presence of the inhibitor and $\Phi_I{}^{-1}$ is the channel-opening equilibrium constant in the presence of the inhibitor (*15*). The equation further assumes that the inhibitor does not affect k_{op} (Figure 5).

REFERENCES

1. Macdonald, R. L., and Olsen, R. W. (1994) $GABA_A$ receptor channels, *Annu. Rev. Neurosci. 17*, 569−602.
2. Kandel, E. R., Schwartz, J. H., and Jessell, T. M. (2000) *Principles of Neural Science*, McGraw-Hill, New York.
3. Mehta, A. K., and Ticku, M. K. (1999) An update on $GABA_A$ receptors, *Brain Res. Rev. 29*, 196−217.
4. Curtis, D. R., and Johnston, G. A. R. (1974) Convulsant alkaloids, in *Neuropoisons, Their Pathophysiological Actions, Poisons of Plant Origin* (Simpson, L. L., and Curtis, D. R., Eds.) Vol. 2, pp 207−248, Plenum Press, New York.
5. Dong, C.-J., and Werblin, F. S. (1996) Use-dependent and use-independent blocking actions of picrotoxin and zinc at the $GABA_C$ receptor in retinal horizontal cells, *Vision Res. 36*, 3997−4005.
6. Rajendra, S., Lynch, J. W., and Schofield, P. R. (1997) The glycine receptor, *Pharmacol. Ther. 73*, 121−146.
7. Etter, A., Cully, D. F., Liu, K. K., Reiss, B., Vassilatis, D. K., Schaeffer, J. M., and Arena, J. P. (1999) Picrotoxin blockade of invertebrate glutamate-gated chloride channels: Subunit dependence and evidence for binding within the pore, *J. Neurochem. 72*, 318−326.
8. Das, P., Bell-Horner, C. L., Machu, T. K., and Dillon, G. H. (2003) The $GABA_A$ receptor antagonist picrotoxin inhibits 5-hydroxytryptamine type 3A receptors, *Neuropharmacology 44*, 431−438.
9. Baulac, S., Huberfeld, G., Gourfinkel-An, I., Mitropoulou, G., Beranger, A., Prud'homme, J.-F., Baulac, M., Brice, A., Bruzzone, R., and LeGuern, E. (2001) First genetic evidence of $GABA_A$ receptor dysfunction in epilepsy: A mutation in the γ2-subunit gene, *Nat. Genet. 28*, 46−48.
10. Wallace, R. H., Marini, C., Petrou, S., Harkin, L., Bowser, D. N., Panchal, R. G., Williams, D. A., Sutherland, G. R., Mulley, J. C., Scheffer, I. E., and Berkovic, S. F. (2001) Mutant $GABA_A$ receptor γ2-subunit in childhood absence epilepsy and febrile seizures, *Nat. Genet. 28*, 49−52.
11. Cossette, P., Liu, L., Brisebois, K., Dong, H., Lortie, A., Vanasse, A., Hilaire, J.-M.-S., Carmant, L., Verner, A., Lu, W. Y., Wang, Y. T., and Rouleau, G. A. (2002) Mutation of GABRA1 in an autosomal dominant form of juvenile myoclonic epilepsy, *Nat. Genet. 31*, 184−189.
12. Scott, R. A., Lhatoo, S. D., and Sander, J. W. A. S. (2001) The treatment of epilepsy in developing countries: Where do we go from here? *Bull. W.H.O. 79*, 344−351.
13. Ramakrishnan, L., and Hess, G. P. (2004) On the mechanism of a mutated and abnormally functioning γ-aminobutyric acid (A) receptor linked to epilepsy, *Biochemistry 43*, 7534−7540.
14. Niu, L., Abood, L. G., and Hess, G. P. (1995) Cocaine: Mechanism of inhibition of a muscle acetylcholine receptor studied by a laser-pulse photolysis technique, *Proc. Natl. Acad. Sci. U.S.A. 92*, 12008−12012.
15. Grewer, C., and Hess, G. P. (1999) On the mechanism of inhibition of the nicotinic acetylcholine receptor by the anticonvulsant MK-801 investigated by laser-pulse photolysis in the microsecond-to-millisecond time region, *Biochemistry 38*, 7837−7846.
16. Jayaraman, V., Usherwood, P. N. R., and Hess, G. P. (1999) Inhibition of nicotinic acetylcholine receptor by philanthotoxin-343: Kinetic investigations in the microsecond time region using a laser-pulse photolysis technique, *Biochemistry 38*, 11406−11414.
17. Hess, G. P., Ulrich, H., Breitinger, H.-G., Niu, L., Gameiro, A. M., Grewer, C., Srivastava, S., Ippolito, J. E., Lee, S. M., Jayaraman, V., and Coombs, S. E. (2000) Mechanism-based discovery of ligands that counteract inhibition of the nicotinic acetylcholine receptor by cocaine and MK-801, *Proc. Natl. Acad. Sci. U.S.A. 97*, 13895−13900.
18. Hess, G. P., Gameiro, A. M., Schoenfeld, R. C., Chen, Y., Ulrich, H., Nye, J. A., Sit, B., Carroll, F. I., and Ganem, B. (2003) Reversing the action of noncompetitive inhibitors (MK-801 and cocaine) on a protein (nicotinic acetylcholine receptor)-mediated reaction, *Biochemistry 42*, 6106−6114.
19. Krivoshein, A. V., and Hess, G. P. (2004) Mechanism-based approach to the successful prevention of cocaine inhibition of the neuronal ($\alpha 3\beta 4$) nicotinic acetylcholine receptor, *Biochemistry 43*, 481−489.
20. Chen, Y., Banerjee, A., and Hess, G. P. (2004) Mechanism-based discovery of small molecules that prevent noncompetitive inhibition by cocaine and MK-801 mediated by two different sites on the nicotinic acetylcholine receptor, *Biochemistry 43*, 10149−10156.
21. Inoue, M., and Akaike, N. (1988) Blockade of γ-aminobutyric acid-gated chloride current in frog sensory neurons by picrotoxin, *Neurosci. Res. 5*, 380−394.
22. Newland, C. F., and Cull-Candy, S. G. (1992) On the mechanism of action of picrotoxin on GABA receptor channels in dissociated sympathetic neurones of the rat, *J. Physiol. 447*, 191−213.
23. Yoon, K.-W., Covey, D. F., and Rothman, S. M. (1993) Multiple mechanisms of picrotoxin block of GABA-induced currents in rat hippocampal neurons, *J. Physiol. 464*, 423−439.
24. Krishek, B. J., Moss, S. J., and Smart, T. G. (1996) A functional comparison of the antagonists bicuculline and picrotoxin at recombinant $GABA_A$ receptors, *Neuropharmacology 35*, 1289−1298.
25. Dillon, G. H., Im, W. B., Carter, D. B., and McKinley, D. D. (1995) Enhancement by GABA of the association rate of picrotoxin and *tert*-butylbicyclophosphorothionate to the rat cloned $\alpha 1\beta 2\gamma 2$ $GABA_A$ receptor subtype, *Br. J. Pharmacol. 115*, 539−545.
26. Shan, Q., Haddrill, J. L., and Lynch, J. W. (2001) A single β subunit M2 domain residue controls the picrotoxin sensitivity of $\alpha\beta$ heteromeric glycine receptor chloride channels, *J. Neurochem. 76*, 1109−1120.
27. Ikeda, T., Nagata, K., Shono, T., and Narahashi, T. (1998) Dieldrin and picrotoxinin modulation of $GABA_A$ receptor single channels, *NeuroReport 9*, 3189−3195.
28. Porter, N. M., Angelotti, T. P., Twyman, R. E., and Macdonald, R. L. (1992) Kinetic properties of $\alpha 1\beta 1$ γ-aminobutyric acid A

receptor channels expressed in Chinese hamster ovary cells: Regulation by pentobarbital and picrotoxin, *Mol. Pharmacol. 42*, 872−881.
29. Udgaonkar, J. B., and Hess, G. P. (1987) Chemical kinetic measurements of a mammalian acetylcholine receptor by a fast-reaction technique, *Proc. Natl. Acad. Sci. U.S.A. 84*, 8758−8762.
30. Hess, G. P., and Grewer, C. (1998) Development and application of caged ligands for neurotransmitter receptors in transient kinetic and neuronal circuit mapping studies, *Methods Enzymol. 291*, 443−473.
31. Milburn, T., Matsubara, N., Billington, A. P., Udgaonkar, J. B., Walker, J. W., Carpenter, B. K., Webb, W. W., Marque, J., Denk, W., McCray, J. A., and Hess, G. P. (1989) Synthesis, photochemistry, and biological activity of a caged photolabile acetylcholine receptor ligand, *Biochemistry 28*, 49−55.
32. Gee, K. R., Wieboldt, R., and Hess, G. P. (1994) Synthesis and photochemistry of a new photolabile derivative of GABA: Neurotransmitter release and receptor activation in the microsecond time region, *J. Am. Chem. Soc. 116*, 8366−8367.
33. Hamill, O. P., Marty, A., Neher, E., Sakmann, B., and Sigworth, F. J. (1981) Improved patch-clamp techniques for high-resolution current recording from cells and cell-free membrane patches, *Pfluegers Arch. 391*, 85−100.
34. Jayaraman, V., Thiran, S., and Hess, G. P. (1999) How fast does the γ-aminobutyric acid receptor channel open? Kinetic investigations in the microsecond time region using a laser-pulse photolysis technique, *Biochemistry 38*, 11372−11378.
35. Chalfie, M., Tu, Y., Euskirchen, G., Ward, W. W., and Prasher, D. C. (1994) Green fluorescent protein as a marker for gene expression, *Science 263*, 802−805.
36. Verdoorn, T. A., Draguhn, A., Ymer, S., Seeburg, P. H., and Sakmann, B. (1990) Functional properties of recombinant rat $GABA_A$ receptors depend on subunit composition, *Neuron 4*, 919−928.
37. Zemkova, H., Vanecek, J., and Krusek, J. (1995) Electrophysiological characterization of $GABA_A$ receptors in anterior pituitary cells of newborn rats. *Neuroendocrinology 62*, 123−129.
38. Gee, K. R., Carpenter, B. K., and Hess, G. P. (1998) Synthesis, photochemistry, and biological characterization of photolabile protecting groups for carboxylic acids and neurotransmitters, *Methods Enzymol. 291*, 30−50.
39. Molnar, P., and Nadler, J. V. (2000) γ-Aminobutyrate, α-carboxy-2-nitrobenzyl ester selectively blocks inhibitory synaptic transmission in rat dentate gyrus, *Eur. J. Pharmacol. 391*, 255−262.
40. Karpen, J. W., and Hess, G. P. (1986) Cocaine, phencyclidine, and procaine inhibition of the acetylcholine receptor: Characterization of the binding site by stopped-flow measurements of receptor-controlled ion flux in membrane vesicles, *Biochemistry 25*, 1777−1785.
41. Goutman, J. D., and Calvo, D. J. (2004) Studies on the mechanisms of action of picrotoxin, quercetin and pregnanolone at the $GABA\rho_1$ receptor, *Br. J. Pharmacol. 141*, 717−727.
42. Gutfreund, H. (1995) *Kinetics for the Life Sciences Receptors, Transmitters and Catalysts*, Cambridge University Press, Cambridge, U.K.
43. Krishtal, O. A., and Pidoplichko, V. I. (1980) A receptor for protons in the nerve cell membrane, *Neuroscience 5*, 2325−2327.
44. Matsubara, N., Billington, A. P., and Hess, G. P. (1992) How fast does an acetylcholine receptor channel open? Laser-pulse photolysis of an inactive precursor of carbamoylcholine in the microsecond time region with BC_3H1 cells, *Biochemistry 31*, 5507−5514.
45. Hammes, G. G. (2000) *Thermodynamics and Kinetics for the Biological Sciences*, p 163, Wiley-Interscience, New York.
46. Twyman, R. E., Rogers, C. J., and Macdonald, R. L. (1989) Pentobarbital and picrotoxin have reciprocal actions on single $GABA_A$ receptor channels, *Neurosci. Lett. 96*, 89−95.
47. Cui, Y., Rajasethupathy, P., and Hess, G. P. (2004) Selection of stable RNA molecules that can regulate the channel-opening equilibrium of the membrane-bound γ-aminobutyric acid receptor, *Biochemistry 43*, 16442−16449.
48. Dupont, L., Dideberg, O., Lamotte-Brasseur, J., and Angenot, L. (1976) Crystal and molecular structure of picrotoxin, $C_{15}H_{16}O_6 \cdot C_{15}H_{18}O_7$, *Acta Crystallogr. B32*, 2987−2993.
49. Cash, D. J., Aoshima, H., and Hess, G. P. (1981) Acetylcholine-induced cation translocation across cell membranes and inactivation of the acetylcholine receptor: Chemical kinetic measurements in the millisecond time region, *Proc. Natl. Acad. Sci. U.S.A. 78*, 3318−3322.
50. Aoshima, H., Cash, D. J., and Hess, G. P. (1981) Mechanism of inactivation (desensitization) of acetylcholine receptor. Investigations by fast reaction techniques with membrane vesicles, *Biochemistry 20*, 3467−3474.

BI0477283